TIME VARIATION OF SiO ($v = 1, J = 2 - 1$) MASERS OF LONG PERIOD VARIABLES

LEE, SANG GAK AND KIM, EUNHYEUK

Department of Astronomy, Seoul National University, Seoul

AND

LEE, HYUNG MOK

Department of Earth Science, Pusan National University, Pusan

ABSTRACT

We have detected a SiO maser line ($v = 1, J = 2 - 1$) for 15 stars out of about 80 long period variables in the wide range of period. No new sources are detected; all detected sources are variables with period longer than 300 days; no evidence is found that the dust grains in the outer envelope have influenced on this line. The time variation of this maser line for 7 stars, T Cep, μ Cep, U Her, R Leo, R Lmi, U Ori, and R Ser is observed and compared with optical light curve at the same epoch of maser observation. No universial relation between the time variation and the optical light curve is found. It implies that the radiation from a central star does not much play an important role for the direct pumping of the SiO maser line.

Key Words : long period variables, SiO maser lines, Pumping Mechanism

I. INTRODUCTION

Although the first detection of the SiO maser line was in the Orion molecular cloud (Synder and Buhl,1974), almost all SiO sources are found to be of late type evolved stars. The observational studies about the SiO masers have been performed in two ways. One is to search the new sources that emitting the SiO masers, and the other is to monitor the time variability. Spencer *et al.* (1981) have observed 46 SiO masers including 13 new sources in $J = 1 - 0$ transition of $v = 1, v = 2, v = 3$ excited states. From an extensive survey of $v = 0$ and $v = 1, J = 1 - 0$ SiO emission of evolved stars by Jewell *et al.* (1991), the large homogeneous SiO observations were obtained for the new and previously detected 155 sources.

The transitions in highly excited states and the maser emissions from isotopes(^{29}SiO and ^{30}SiO) were also reported. Cernicharo *et al* (1993) have detected the SiO emission of $v = 4, J = 5 - 4$ of VY CMa including the emission from $J = 1 - 0$ to $J = 6 - 5$ of $v = 1, v = 2$ and $v = 3$. They also observed the isotopic emission of SiO for the same object (Cernicharo and Bujarrabal 1992). Alcolea and Bujarrabal (1992) have studied the variation of ^{29}SiO maser, that has been found to be similiar to that of $v = 1, 2$ ^{28}SiO ones.

The first systematic study on the variability of the SiO masers was made by Hjalmarson and Olofsson (1979). They observed $J = 2 - 1, v = 1$ transition in the Mira-type variables, o Cet and R Leo, and star-forming region Ori A. They claimed that the SiO fluxes from R Leo and o Cet appeared to be correlated with their near-infrared intensities, having a distinct phase lag with respect to the visual light curve. This work was continued by Nyman and Olofsson (1985,1986). These authors observed the variability of SiO maser in $J = 2 - 1$ of $v = 0$ and $v = 1$ for eight Mira variables. However, their long-spaced monitoring did not give significant results except the large amount of variations of maximum SiO intensity and dynamic range (maximum/minimum intensity) between different periods and between different sources. A long-term short-spaced monitoring of the SiO maser was performed by Martinez *et al.* (1988). They observed three supergiants, two irregular variables, nine Mira variables and the star-forming

region Ori A every 20 $\sim$ 30 days. They argued that there were missing maxima, i.e. maximum confused with the emission of the adjacent minima, and that the time variations of the SiO emission had a phase lags of 0.1 $\sim$ 0.2 relative to the visual maxima. Such a phase difference between the SiO maser line intensity and the visual light curve per every cycle indicates that stellar radiation could play an important role for pumping the maser line. It was found that there was a good correlation between SiO maser line intensity and infrared $8\mu m$ flux(Bujarrabal *et al* 1987).

Through interferometric observations, it has been known that the SiO maser region is close to the the central stars(Hollis *et al.* 1990; Colomer *et al.* 1992), typically $\sim 2 - 6R_*$ with a maser size ranging from $10^{12} \sim 10^{13} cm$ for LPV to $10^{13} \sim 10^{14} cm$ for supergiants. Unlike OH and H_2O, this maser cannot reside in the expanding wind.It alluded that collision had also an important role for pumping the maser line because of a plenty of hydrogen molecules in this region. For most of sources which investigated by Martinez *et al.* (1988) the repetitiveness of the SiO curves was found relatively poor and the SiO maser emission varied roughly following the IR variability. However, there was no ccorrelation between the average SiO and IR amplitude. Moreover, the relation between IR $8\mu m$ flux and intensity of SiO maser line can be interpreted by Vardya *et al.* (1986) that the emission line at $\sim 8\mu m$ of IRAS LRS spectra due to vibrational transition of SiO molecule was pumped by collision, and supported the collisional pump model of Elitzer (1980).

Theoretical calculations by both collision and radiation are in principle capable of pumping the SiO masers. Kwan and Scoville(1974) showed that the radiation worked faster than the collision. But using the updated value of Bieniek and Green's(1983) for the collisional cross-section, Lockett and Elitzur(1992) proved that the collisional pumping would be even more probable. We also perfomed the similiar calculation and got the same results of Lockett and Elitzur(Kim and Lee 1994) that the collisional pumping could produce the strongest emission. However, we could not get a sufficient pumping to match the observed line intensity, since we used an expanding envelope model for the SiO maser. The observational and theoretical knowledge on the SiO maser phenomenon is therefore still controversial.

Since the real period of the optical light variation for the late type stars varies from period to period, the correlation between the optical variation and the maser line variation should be investigated by the simultaneous observations of the both wavelength regions. In this study, we compare our maser observation data with the optical light curve at the same time of the our maser observation. Those optical data are kindly provided by AAVSO(Mattei 1993). We present the observational procedure in Section II and a general discussion on the observed data in Section III. The results are summarized in Section IV.

II. OBSERVATION

We have observed $v = 1, J = 2 - 1$ transition of the SiO molecule for about 80 stars with various periods, which were selected from General Catalog of Variable Stars (GCVS). The list of sources is presented in Table 1 with their name, coordinate, period and spectral type.

The observations have been made from Apr. 1992 to Nov. 1993, using DRAO(Daeduk Radio Astronomical Observatory) 14m radio telescope. The receiver was a 85-115 GHZ, cooled, single-channel Schottky mixer. The system temperature was typically 600-800 K. To get the information about the intensity variability we have observed each of them once a month approximately. An except for the summer season, since the telescope time is not available to maintenance. At the frequency 86 GHz the beam size, aperture efficiency and beam efficiency of the DRAO 14m telescope were $69''$, 0.38 and 0.50 respectively. For the backend, a 256 channel filter bank with a resolution of 250 kHz, corresponding to the velocity resolution of $\Delta v \sim 0.6 km/sec$ was used. We used only the filter bank because its noise was less than that of the autocorrelator and our concern was concentrated to only the time variability of the intensity.

The pointing problem of the radio telescope have bothered many observers. In order to check the pointing accuracy we have used the well-known a five point two dimensional Gaussian fitting method. For any one point that the telescope directed we got the line profile of the extra four points which have about $30''$ offsets from the initial point.

After that we have performed two dimensional Gaussian fitting, using the intensities of five points. Then we

Table 1: Objects

Name	α_{1950}	δ_{1950}	Period	Sp. Type	Name	α_{1950}	δ_{1950}	Period	Sp. Type
R And	00 21 23	+38 18 00	409.33	S3,5e-S8,8e(M7e)	W Aql	19 12 42	-07 08 06	490.43	S3,9e-S6,9e
V845 Aql	20 26 49	+00 40 48	228.50		RZ Ari	02 53 00	+18 07 48	30.00	M6III
R Aur	05 13 15	+53 31 54	457.51	M6.5e-M9.5e	W Boo	14 41 13	+26 44 24	450.00	M2-M4III
BY Boo	14 05 56	+44 05 30		M4-4.5III	VZ Cam	07 20 41	+82 30 48	23.70	M4IIIa
X Cnc	08 52 34	+17 25 24	195.00	C5,4(N3)	BO Cnc	08 49 28	+28 26 54		M3III
BP Cnc	08 23 58	+12 49 18	40.00	M3III	R Cvn	13 46 48	+39 47 24	328.53	M5.5e-M9e
TU Cvn	12 52 40	+47 28 06	50.00	M5III	AG Cap	21 43 36	-09 30 24	25.00	M3III
R Cas	23 55 52	+51 06 36	430.46	M6e-M10e	T Cas	00 20 31	+55 30 54	444.83	M6e-M9.0e
MP Cas	23 18 34	+60 55 54	338.00	M8	T Cep	21 08 53	+68 17 12	388.14	M5.5e-M8.8e
μ Cep	21 41 59	+58 33 00	730.00	M2eIa	T Cet	00 19 15	-20 20 06	158.90	M5-6SIIe
U Cet	02 31 20	-13 22 00	234.76	M2e-M9e	AD Cet	00 11 54	-08 03 30		M3III
o Cet	02 16 49	-03 12 12	331.96	M5e-M9e	S Crb	15 19 22	+31 32 48	360.26	M6e-M8e
R Cyg	19 35 29	+50 05 12	426.45	S2.5,9e-S6,9e(Tc)	T Cyg	20 45 11	+34 11 24		K3III
U Cyg	20 18 03	+47 44 12	463.24	C7,2e-C9,2(Npe)	RT Cyg	19 42 13	+48 39 24	190.28	M2e-M8.8eIb
BG Cyg	19 36 59	+28 23 42	288.00	M7e-M8e	V640 Cyg	21 37 18	+40 58 00	222.00	
χ Cyg	19 48 38	+32 47 12	408.05	S6,2e-S10,4e(MSe)	EU Del	20 35 38	+18 05 30	59.70	M6.4III
R Dra	16 32 31	+66 51 30	245.60	M5e-M9eIII	Y Dra	09 36 49	+78 04 48	325.79	M5e
UX Dra	19 23 22	+76 27 42	168.00	C7,3(NO)	CQ Dra	12 27 56	+69 28 42		M3IIIa
DM Eri	04 38 15	-19 46 00	30.00	M4III	R Gem	07 04 21	+22 46 54	369.91	S2.9e-S8.9e(Tc)
η Gem	06 11 52	+22 31 24	232.90	M3IIIab	U Her	16 23 35	+19 00 18	406.10	M6.5e-M9.5e
RU Her	16 08 09	+25 12 00	484.83	M6e-M9	OP Her	17 55 22	+45 21 24	120.50	M5IIb-IIIa(S)
V636 Her	16 45 44	+42 19 36		M4III-IIIa	R Hya	13 26 58	-23 01 24	388.87	M6e-M9es(Tc)
T Hya	08 53 14	-08 57 00	298.70	M3e-M9:e	R Leo	09 44 52	+11 39 42	309.95	M6e-M8IIIe-M9.5e
VY Leo	10 53 26	+06 27 12		M5.5III	DE Leo	10 22 37	+09 02 24		M2IIIabs
R Lmi	09 42 35	+34 44 36	372.19	M6.5e-M9.0e(Tc:)	R Lep	04 57 20	-14 52 48	427.07	C7,6e(N6e)
RX Lep	05 09 30	-11 54 36	60.00	M6.2III	R Lyr	18 53 49	+43 52 48	46.00	M5III
V Mon	06 20 12	-02 10 12	340.50	M5e-M8e	X Oph	18 35 57	+08 47 18	328.85	M5e-M9e
κ Oph	16 55 18	+09 27 06		K2III	U Ori	05 55 51	+20 10 06	368.30	M6e-M9.5e
CK Ori	05 27 41	+04 10 00	120.00	K2IIIe:	S Peg	23 18 01	+08 38 42	319.22	M5e-M8.5e
Z Peg	23 57 33	+25 36 30	334.80	M6e-M8.5e(Tc)	GZ Peg	23 07 00	+08 24 24	92.66	M4sIII
ρ Per	03 01 58	+38 38 54	50.00	M4IIb-IIIa	R Psc	01 28 03	+02 37 30	344.50	M3e-M6e
TV Psc	00 25 26	+17 37 00	49.10	M3III-M4IIIb	KK Sge	19 09 04	+17 46 48	438.00	M7
R Ser	15 48 23	+15 17 00	356.41	M5IIIe-M9e	S Ser	15 19 19	+14 29 36	371.84	M5e-M6e
τ Ser	15 34 09	+15 15 54	100.00	M5IIb-IIIa	TU Tau	05 42 10	+24 24 00	190.00	C5,4(N3)+A2III-V
CE Tau	05 29 17	+18 33 30	165.00	M2Iab-Ib	R Tri	02 34 00	+34 02 54	266.90	M4IIIe-M8e
R UMa	10 41 08	+69 02 18	301.62	M3e-M9e	T UMa	12 34 07	+59 45 42	256.60	M4IIIe-M7e
Z UMa	11 53 54	+58 09 00	195.50	M5IIIe	VY UMa	10 41 37	+67 40 30		C6,3(No)
CO UMa	11 06 34	+36 34 54		M3.5IIIab	RR UMi	14 56 47	+66 07 54	43.30	M5III
R Vir	12 35 58	+07 15 48	145.63	M3.5IIIe-M8.5e	S Vir	13 30 24	-06 56 18	375.10	M6IIIe-M9.5e
ET Vir	14 08 06	-16 04 00	80.00	M2IIIa	FW Vir	12 35 49	+02 07 48	15.00	M3IIIab

corrected the the direction of telescope by the amount of the fitted results. But to confirm the signal we had to reduce the noise temperature below the typical value ($\sim 0.05K$). So the large integration time caused the pointing error corresponds to some 20 $\sim$ 30% error in most observed line intensities. The intensity variation due to the telescope's elevation has been ignored since it is very small.

Because of the polarization we would expect that the intensity and line profile shape of maser line would vary from position to position in the celestial sphere(Clark et al. 1982). To remove such an effect our observations have been made at the nearly same local siderial time. The observing log is presented in Table 2.

III. OBSERVATIONAL RESULTS

(a) Characteristics of stars detected SiO maser line

For 15 sources among the 80 program stars we have detected maser line with 14m DRAO radio telescope. The periods of all detected sources are longer than 300 days as shown in the period distribution of the program stars of

Table 2: Observing Log

Observing date	# of stars	T_{noise} [K]
1992/03/28	8(3)[a]	0.094
1992/04/23	31(12)	0.056
1992/05/23	19(6)	0.092
1992/10/31	19(6)	0.089
1992/12/05	22(7)	0.078
1992/12/27	25(11)	0.072
1993/01/22	43(11)	0.065
1993/02/24	42(12)	0.094
1993/04/03	13(10)	0.050
1993/10/09	7(6)	0.058
1993/10/31	13(12)	0.042
1993/11/21	9(9)	0.042

[a]The values in the parenthesis represent the number of stars where the SiO maser line is detected.

Figure 1. The spectral types of these stars are of M type except for the χ Cyg which is S type.

The asymmetric factor of the optical light curve, f value, which was defined by the rise time divided by the period, has been found to be related with the OH maser strength(Bowers, 1975). From the analysis of far-IR excess($S_{60\mu m}/S_{3.5\mu m}$), Onaka et al(1989) showed that the more far-IR excess was the less the f value was and that the strength of OH maser line was strongly dependent on the dust grain around the star.

The f values based on the light curve data of AAVSO during the same period of the maser observation for this study, were calculated for 28 stars which were belong to both two groups (maser detected and non-detected) and presented in Figure 2. We can not find any distributional difference for the two groups in Figure 2. The detection of the SiO maser line does not depend on the f value, which means that it is not related with the far-IR radiation of the dust grain.

The colors, $log(S_\lambda(12\mu m)/S_\lambda(25\mu m))$ and $log(S_\lambda(25\mu m)/S_\lambda(60\mu m))$ for the 58 program stars were estimated from the IRAS point source data and they are listed in the Table 3 along with the f value. It is also found that there is no difference between two groups in the color-color diagram of Figure 3.

(b) Intensity variation of SiO maser line

The antenna temperature (T_A^*), velocity-integrated flux ($\int T_A^* dv$), noise, velocity with respect to LSR at the peak and the elevation at the observation are presented in Table 4 for the 15 maser detected stars. Among them, the variations of the SiO maser line are searched for these with more than 8 maser observations. The time variation of the antenna temperature and velocity-integrated flux of maser line for T Cep, μ Cep, U Her, R Leo, R Lmi, U Ori and R Ser is shown in Figure 4 with the AAVSO light curve of the same epoch.

It has been known that the maximum SiO intensity varies by a large amount from cycle to cycle and the dynamic range varies between different cycles and between different sources (Nyman and Olofsson 1986). Our maser line data and the AAVSO visual data can only cover one or one and half cycle. We therefore compare them directly.

For the T Cep, the maximum intensity of the maser line appears at the optical maximum, but the next maximum, which is expected at JD-2448200 ～ 1100 does not exist. People sometimes call it as "missing maxima" (Martinez et al 1988). The missing maxima may be due to the small dynamic range in this particular epoch, since T Cep showed a good periodicity at their normalized SiO integrated flux curves of Nyman and Olofsson (1986). However, they showed the SiO maximum laged the optical maximum by 0.1 ～ 0.2 phase, while the SiO minimum occured later than 0.7 phase. But our data show that the maser maximum occured around the maximum of the optical
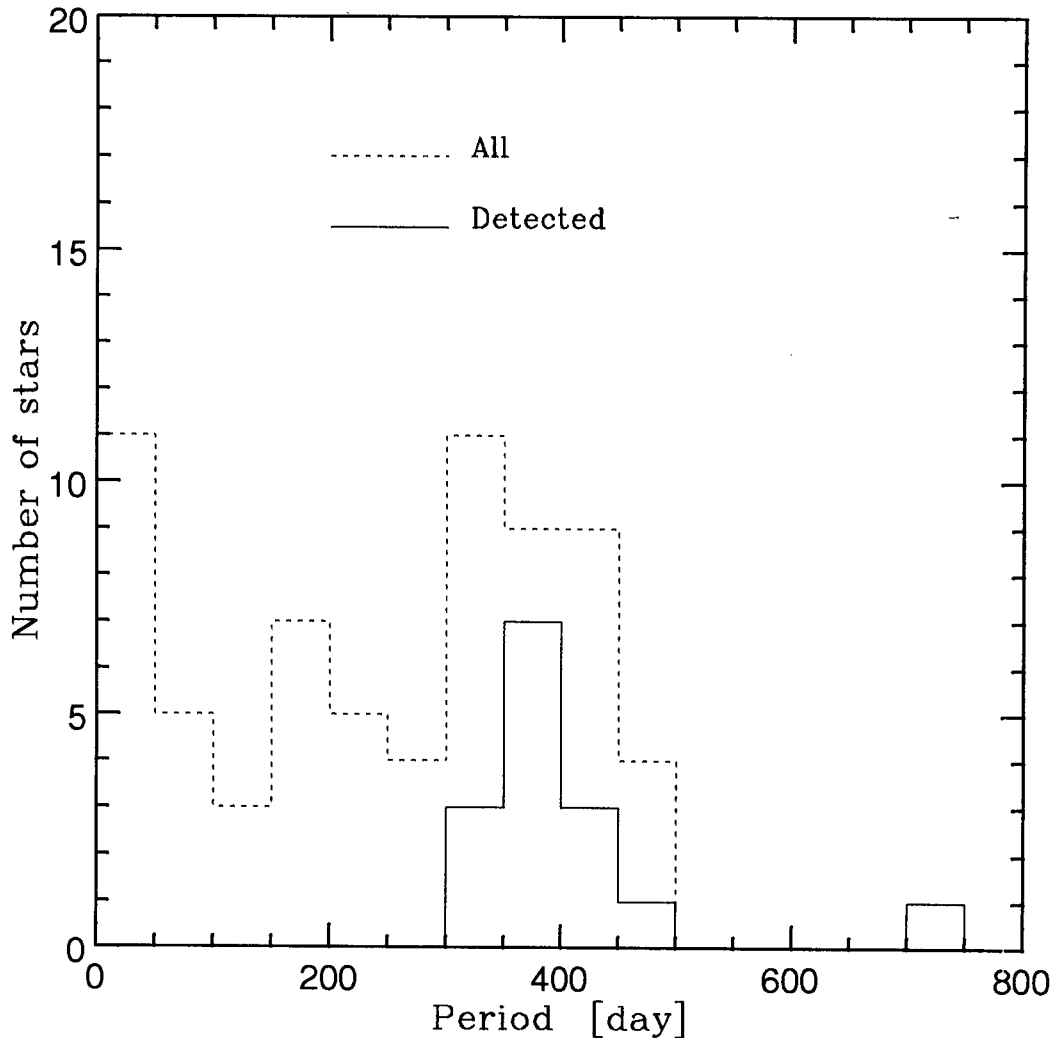
Fig. 1 : Period distribution of observed stars. The solid line presents the the distribution of stars where the maser line was detected and the dotted line presents the distribution for all the stars except for the irregular variables. Note the presence of a sharp cut-off.

light. This suggests a possibility that even the phase lag may varies from cycle to cycle for T Cep. For μ Cep unlike others which is a supergiant with period of $\sim$ 730 days, we have found that the variation of the maser line is quite different from the optical light curve. We can not find any correlation between the rapid and erratic variation of the maser line and the slowly and smoothly varing optical light. The maser maximum at JD-2448202 $\sim$ 760 day would give a maser period of $\sim$ 300 days, which is less than the half of the optical period. For U Her, two maxima and two minima of the maser line suggest a period of $\sim$ 300 day, while the optical curve of this epoch gives the optical period longer than $\sim$ 400 day, which is about the same as the known average optical period of this star. Therefore this implies that the maser line period is different from the optical period for U Her, if the periodicity of the maser line is present. For R Leo, the variation pattern of the maser line is similar to that of T Cep. However, Nyman and Olofsson (1896) could not find any periodicity of maser line from its considerably erratic variations of their maser data. But our data can give $\sim$ 320 days of the maser period with $\sim$ 0.3 phase lag from the optical peak,
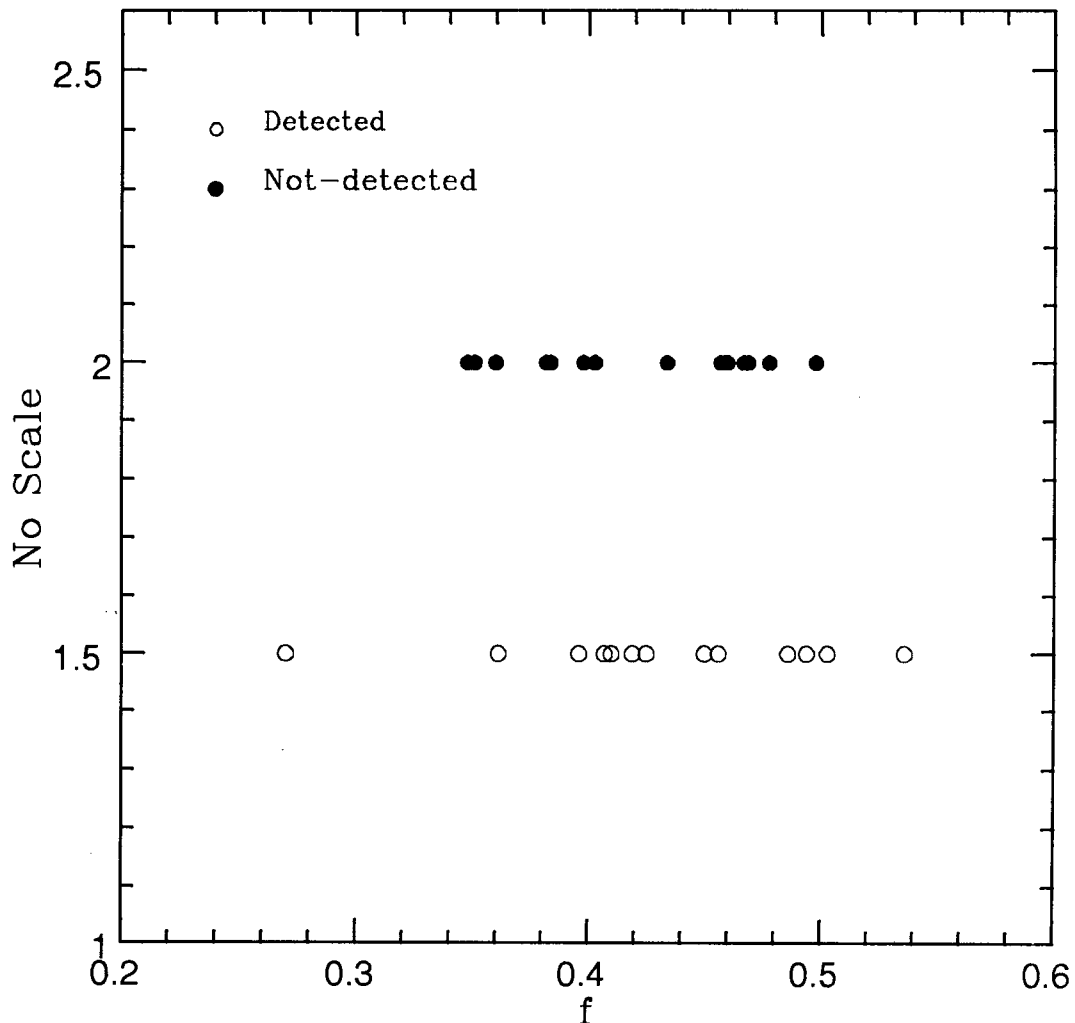
Fig. 2 : The distribution of f value. The open circles refer to the detected stars, and the filled circles, to the non-detected stars. There is a significant difference between the two groups.

if we assume that the peak intensity and the dynamic range vary from cycle to cycle, as they did. In the case of R Lmi, the period of the maser line seems to be less than ~ 250 days, which is about two third of the optical period of ~ 370 days. For U Ori, we could infer the period of maser line as ~ 310 days from its two maxima at JD-2448200 ~ 770 day and ~ 1080 day, which is about the same as that of optical light (~ 330 days) with ~ 0.2 phase difference between the maxima of the maser line and optical light. The similar maser periodicity and the phase lag for this star has been found by Nyman and Olofsson (1986). For R Ser, the maser intensity at the near optical maxima is about the same as that of the near optical minimum. It is difficult to find any correlation between the maser line variation and the optical light curve.

All presented here imply that there is no universal relation between the SiO maser variation and the optical light curve. In this study only U Ori out of 7 stars shows that its maser line varies with about the same period of the light curve and with the same (~ 0.2) phase lag as that of the previous study. T Cep seems to have a phase lag
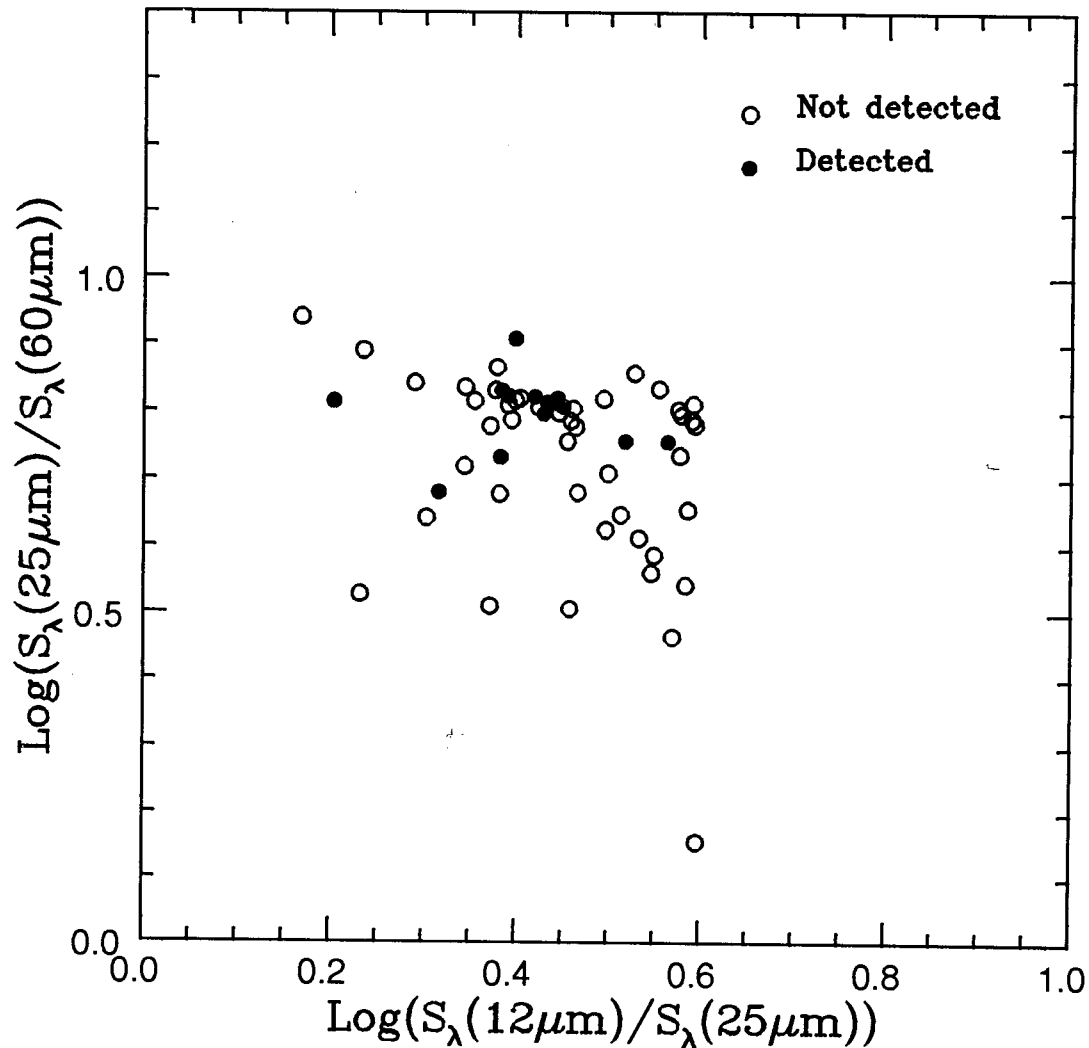
Fig. 3 : The IR color-color diagram of the two groups. The filled circles refer to the detected stars and the open circles, to the the detected stars, if the IR radiation plays an important role for the pumping of the SiO maser. However, the actual distribution of the two groups seem quite similar.

variation and μ cep, U Her and R Lmi seem to have different periodicities of their maser line from those of optical light. R Leo, which has not shown any periodicity of the maser line, is found to have a variation with the optical period and ~ 0.3 phase lag in our data. And no relation is found for R Ser. Therefore we can conclude that for most cases, the radiation from the central star could not directly affect the SiO maser variation.

(c) Variation of peak velocity of SiO maser line

The interferometry by Colomer *et al.* (1992) shows that the observed maser spot sizes are rather compact. Several evidences, such as no correlation between the expanding wind and the SiO maser activity, low mass-loss rates in the stars which were detected $v = 3$ maser line, suggested that masers are located in the region whose density is
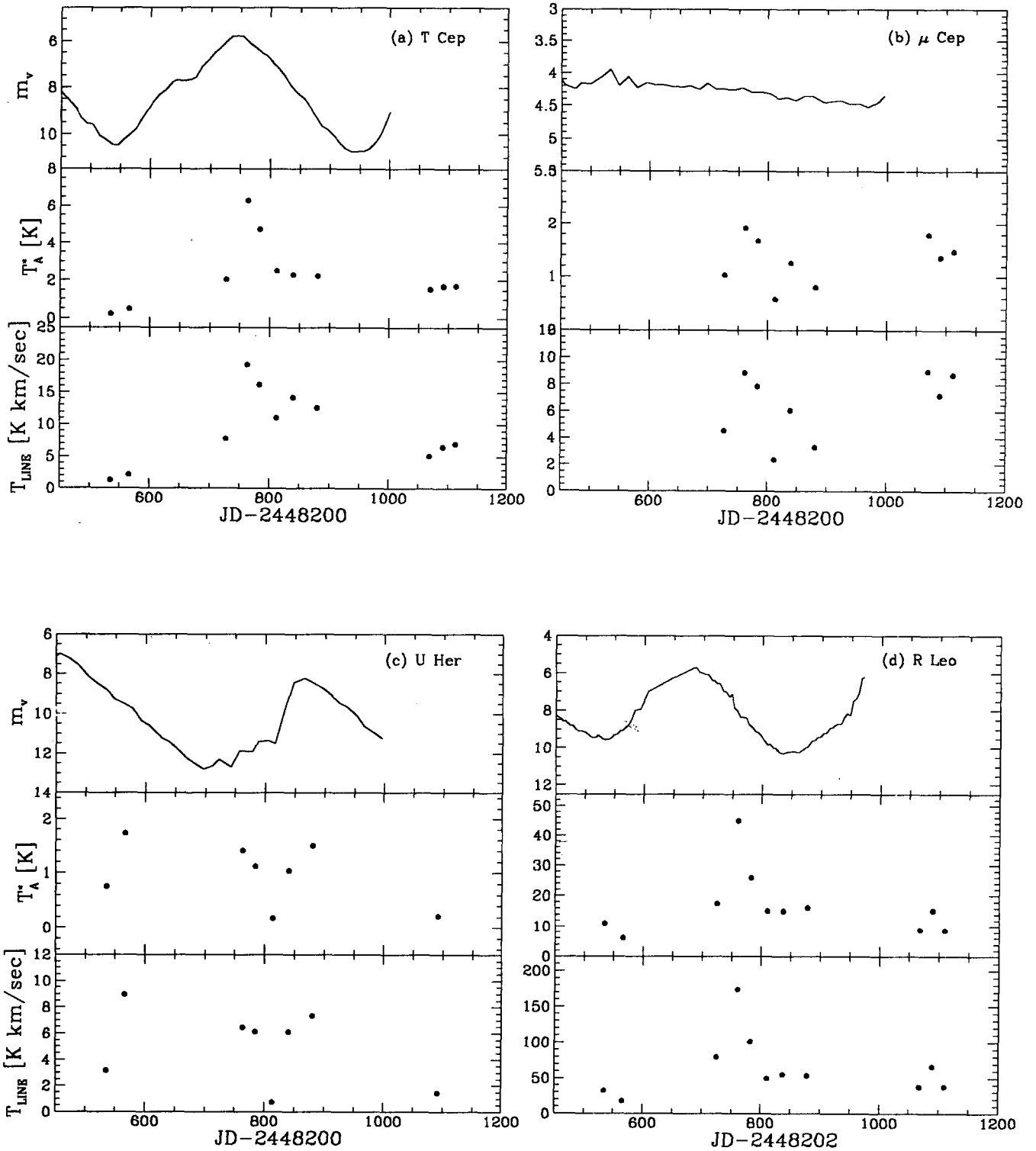
Fig. 4 : Time variation of the optical light, peak intensity and velocity-integrated intensity of 7 LPVs; (a) T Cep, (b) μ Cep, (c) U Her, (d) R Leo, (e) R Lmi, (f) U Ori, and (g) R Ser. From top to bottom panels, the visual light curve, the variation of peak intensity, and the velocity-integrated intensity, respectively.

(e) R Lmi

(f) U Ori

(g) R Ser

Fig. 4 : Continued
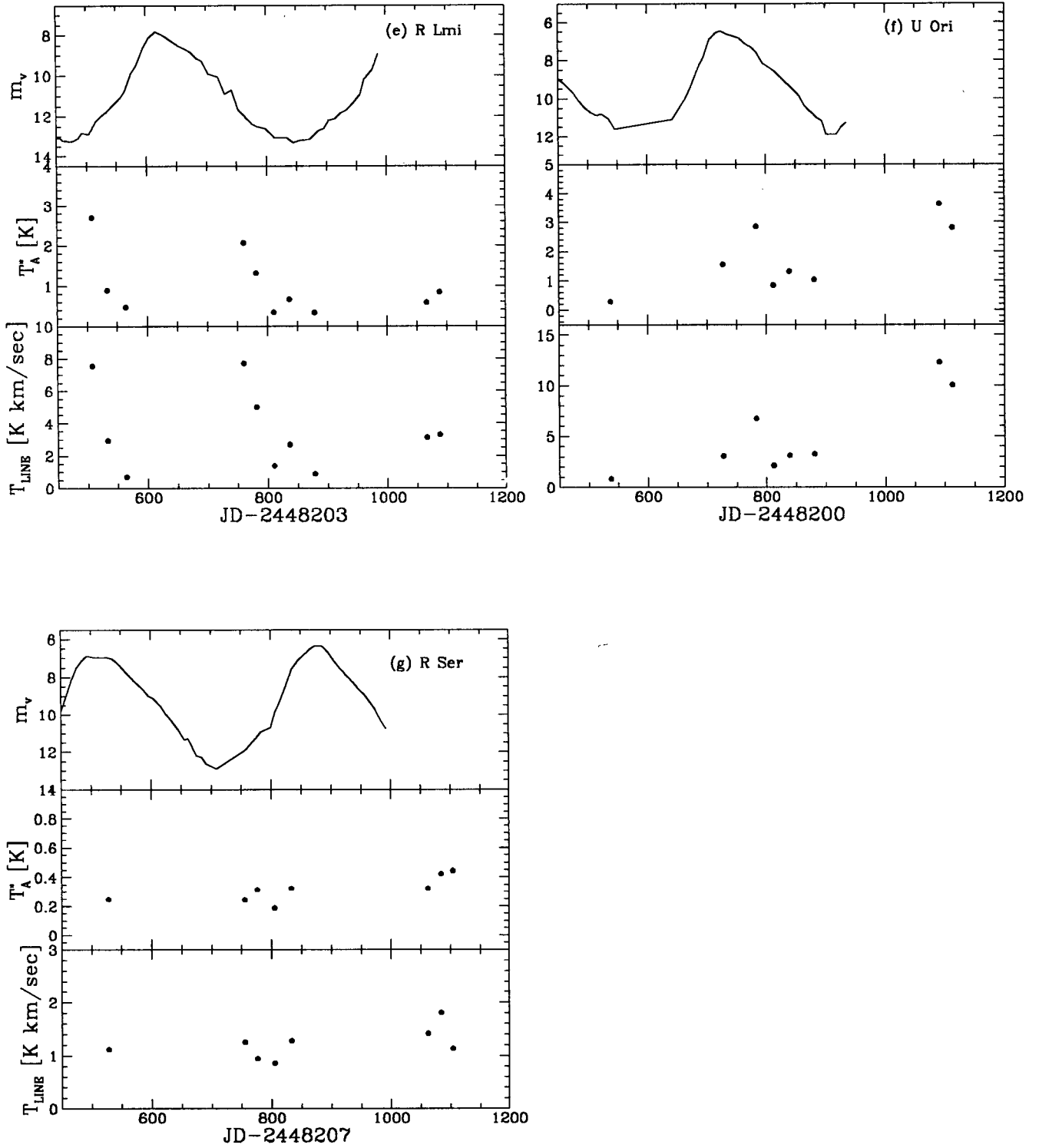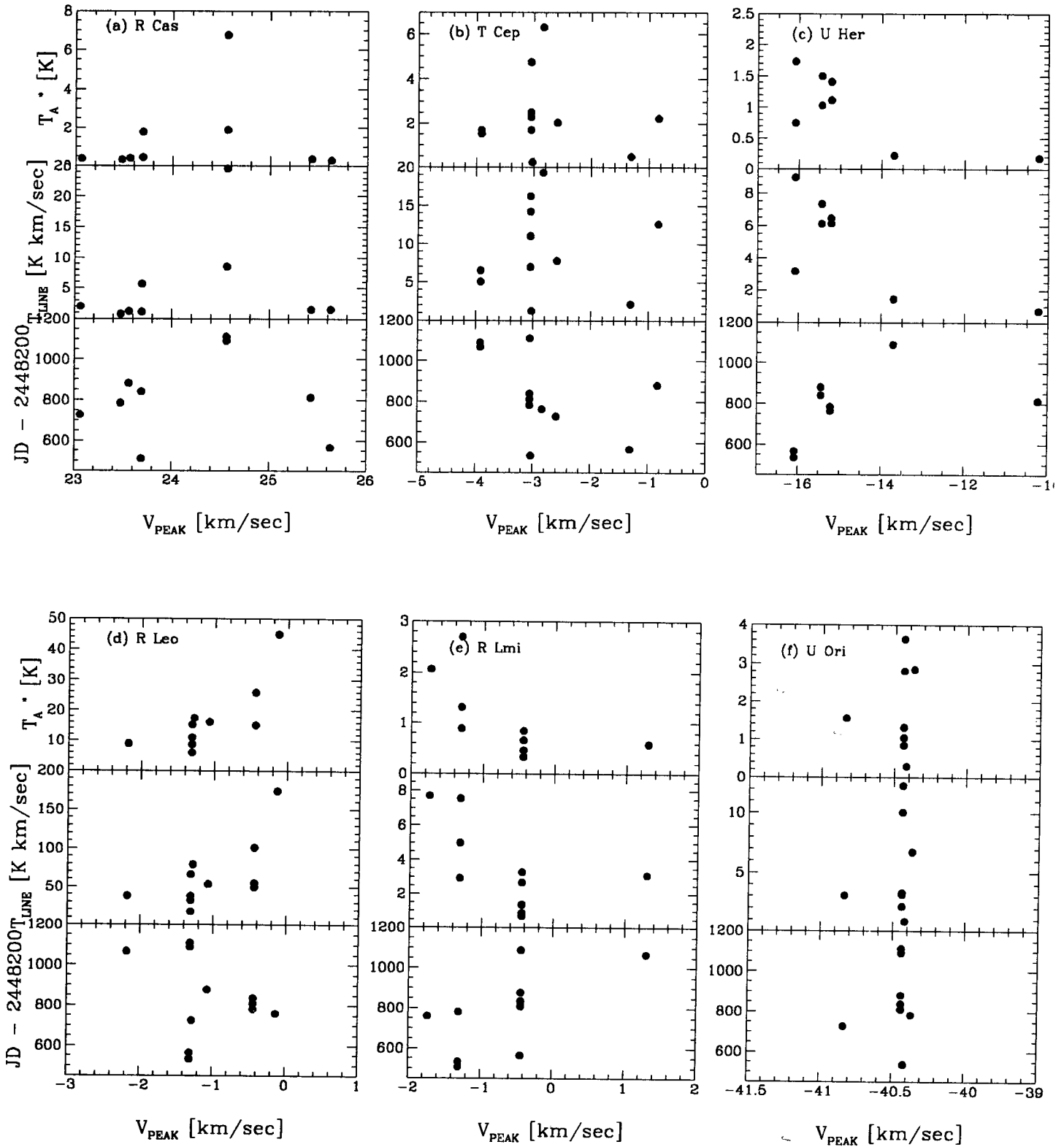
Fig. 5 : Variations of the peak velocity. The variation of the peak velocity with respect to the peak intensity, velocity-integrated intensity, and the time for 6 LPVs (a) R Cas, (b) T Cep, (c) U Her, (d) R Leo, (e) R Lmi, and (f) U Ori are presented. Note their small variation for all stars. See the text.

Table 3: IR colors and f values of selected stars

Name	f value	$12 - 25^a$	$25 - 60^b$	Name	f value	$12 - 25^a$	$25 - 60^b$
R And	0.40	0.290	0.841	U Her	0.41	0.204	0.814
W Aql	0.38	0.371	0.778	RU Her	0.46	0.344	0.836
V845 Aql		0.168	0.940	OP Her		0.500	0.709
RZ Ari		0.594	0.780	R Hya	0.54	0.454	0.764
R Aur	0.49	0.399	0.908	T Hya		0.459	0.786
W Boo		0.591	0.787	R Leo	0.43	0.519	0.756
VZ Cam		0.592	0.811	R Lmi	0.42	0.385	0.830
X Cnc		0.547	0.561	R Lep		0.514	0.647
R Cvn	0.47	0.403	0.819	RX Lep		0.355	0.815
TU Cvn		0.579	0.795	R Lyr		0.578	0.735
R Cas		0.451	0.807	V Mon	0.50	0.467	0.680
T Cas		0.379	0.865	X Oph	0.49	0.445	0.819
T Cep	0.50	0.447	0.810	U Ori	0.40	0.420	0.821
μ Cep		0.317	0.680	CK Ori		0.597	0.156
U Cet		0.455	0.756	S Peg	0.48	0.450	0.798
o Cet	0.27	0.334	0.876	Z Peg	0.43	0.377	0.831
S Crb	0.36	0.391	0.823	R Psc		0.343	0.719
R Cyg	0.38	0.303	0.642	TV Psc		0.528	0.857
T Cyg		0.586	0.654	R Ser	0.45	0.383	0.732
U Cyg	0.46	0.498	0.625	S Ser		0.372	0.511
RT Cyg		0.462	0.804	TU Tau		0.584	0.543
BG Cyg		0.424	0.806	CE Tau		0.495	0.819
640 Cyg		0.232	0.529	R Tri	0.46	0.465	0.777
χ Cyg		0.565	0.755	R UMa	0.35	0.235	0.890
EU Del		0.555	0.834	T UMa		0.382	0.678
R Dra	0.47	0.391	0.809	Z UMa		0.395	0.787
Y Dra	0.36	0.398	0.816	VY UMa		0.570	0.465
UX Dra		0.533	0.613	RR UMi		0.576	0.803
R Gem	0.35	0.458	0.507	S Vir	0.46	0.434	0.813

$^a12 - 25$ presents the color, $log(S_{12\mu m}/S_{25\mu m})$.
$^b25 - 60$ presents the color, $log(S_{25\mu m}/S_{60\mu m})$.

unrelated to the mass-loss rate. It is believed that SiO maser emission originates in large blobs, or emission cells that were formed in the extended atmosphere between the photosphere and the dust formation point.

So we have tested if there is any correlation between the velocity at the peak intensity and the line intensity. If this SiO maser is formed in the expanding envelope and its intensity depends upon the mass-loss rate, we would expect to find some relation between the peak velocity and the line intensity.

The variation of the peak velocity with time, flux and peak intensity variation with respect to the velocity for R Cas, T Cep, U Her, R leo, R Lmi, and U Ori are presented in Figure 5. The peak velocity variations for these stars are found to be $\sim 3km/sec, \sim 3km/sec, \sim 6km/sec, \sim 2km/sec, \sim 5km/sec$, and $\sim 1km/sec$ respectively. These small variations are consistent with the fact that the maser pumping region is restricted to a small region. And the random distribution of the peak velocity versus intensity diagram implies that the maser is not related to the velocity field of the region. These results are consistent with the inference that the SiO maser is formed in the small regions and poorly correlated with the expansion velocity of the circumstellar shell.

LEE, KIM AND LEE

Table 4: Intensity variation of detected sources

Name	Observing date	T_A^*	$\int T_A^* dv$	ΔT	V_{PEAK}	Elevation
χ Cyg	1993/02/24	1.29	4.26	0.057	12.60	68.4
	1993/10/31	1.50	6.35	0.039	12.17	53.2
R Ser	1992/04/23	0.25	1.12	0.033	33.23	68.4
	1992/12/05	0.25	1.25	0.051	33.92	64.9
	1992/12/27	0.31	0.95	0.053	34.56	47.1
	1993/01/22	0.19	0.86	0.058	34.56	57.6
	1993/02/24	0.32	1.28	0.057	35.43	66.5
	1993/10/09	0.32	1.42	0.048	31.30	65.3
	1993/10/31	0.42	1.81	0.048	31.09	68.2
	1993/11/21	0.44	1.14	0.050	31.30	56.8
R Aur	1992/04/23	0.37	0.41	0.073	−3.04	59.4
μ Cep	1993/10/31	1.03	4.51	0.055	26.54	64.0
	1992/12/05	1.92	8.86	0.070	26.96	67.4
	1992/12/27	1.68	7.87	0.059	26.96	66.5
	1993/01/22	0.58	2.37	0.062	27.17	66.7
	1993/02/24	1.25	6.06	0.053	26.96	65.3
	1993/04/03	0.80	3.31	0.053	26.57	59.3
	1993/10/09	1.79	8.97	0.159	26.30	46.7
	1993/10/31	1.36	7.20	0.054	26.30	52.0
	1993/11/21	1.49	8.71	0.026	26.30	49.8
o Cet	1992/12/27	0.31	0.98	0.060	46.96	46.2
	1993/10/31	0.75	2.78	0.035	46.09	47.9
	1993/11/21	1.18	4.01	0.028	46.09	43.7
R Cas	1992/03/28	1.78	5.70	0.066	23.70	53.0
	1992/05/23	0.29	1.57	0.107	25.63	64.5
	1992/10/31	0.39	2.05	0.075	23.07	34.2
	1992/12/27	0.33	0.81	0.063	23.48	66.4
	1993/01/22	0.37	1.55	0.064	25.43	74.8
	1993/02/24	0.45	1.16	0.063	23.70	70.5
	1993/04/03	0.41	1.24	0.038	23.57	62.3
	1993/10/31	6.75	24.56	0.041	24.57	47.2
	1993/11/21	1.88	8.55	0.137	24.57	69.6
T Cep	1992/04/23	0.24	1.28	0.049	−3.02	56.3
	1992/05/23	0.50	2.18	0.100	−1.30	56.6
	1992/10/31	2.05	7.82	0.061	−2.58	57.2
	1992/12/05	6.31	19.31	0.093	−2.83	57.0
	1992/12/27	4.75	16.21	0.063	−3.04	57.6
	1993/01/22	2.51	11.04	0.078	−3.04	56.8
	1993/02/24	2.31	14.25	0.056	−3.04	57.1
	1993/04/03	2.24	12.64	0.038	−0.83	57.5
	1993/10/09	1.54	5.09	0.096	−3.91	51.0
	1993/10/31	1.70	6.55	0.029	−3.91	56.7
	1993/11/21	1.71	7.02	0.025	−3.04	57.1
S Vir	1992/12/05	0.41	1.48	0.157	8.70	44.7
	1993/01/22	0.35	1.37	0.061	8.25	43.6
X Oph	1992/04/23	0.15	0.75	0.030	−54.35	61.7
	1992/05/23	0.20	0.89	0.070	−53.44	61.2
	1992/10/31	0.29	1.81	0.052	−56.48	60.9
	1993/02/24	0.25	0.78	0.052	−55.65	62.4
	1993/04/03	0.18	0.80	0.053	−54.57	59.7

Table 4: Continued

Name	Observing date	T_A^*	$\int T_A^* dv$	ΔT	V_{PEAK}	Elevation
U Ori	1992/04/23	0.29	0.85	0.093	−40.41	51.4
	1992/10/31	1.56	3.08	0.136	−40.83	67.7
	1992/12/27	2.85	6.76	0.055	−40.37	71.1
	1993/01/22	0.85	2.14	0.074	−40.43	65.1
	1993/02/24	1.32	3.14	0.102	−40.43	71.8
	1993/04/03	1.05	3.29	0.033	−40.43	65.5
	1993/10/31	3.63	12.31	0.038	−40.43	72.9
	1993/11/21	2.81	10.07	0.035	−40.43	72.9
U Her	1992/04/23	0.75	3.18	0.032	−16.08	64.4
	1992/05/23	1.73	8.98	0.073	−16.08	72.3
	1992/12/05	1.41	6.46	0.089	−15.21	52.4
	1992/12/27	1.12	6.14	0.208	−15.21	56.5
	1993/01/22	0.19	0.75	0.065	−10.22	63.8
	1993/02/24	1.04	6.13	0.055	−15.43	60.1
	1993/04/03	1.50	7.34	0.052	−15.43	61.7
	1993/10/31	0.22	1.46	0.044	−13.70	53.2
R Hya	1992/03/28	2.14	4.97	0.280	−28.08	30.5
	1992/04/23	0.40	2.32	0.048	−13.47	30.4
	1992/12/27	0.53	1.57	0.067	−10.86	30.1
	1993/01/22	1.33	2.99	0.077	−10.01	30.3
	1993/02/24	1.04	3.04	0.027	−10.45	30.3
	1993/10/31	0.81	3.77	0.079	−9.57	29.6
	1993/11/21	1.05	4.11	0.044	−8.96	27.6
S Crb	1992/04/23	0.19	0.48	0.080	−0.43	59.1
	1992/12/27	0.42	1.43	0.061	2.17	67.0
	1993/02/24	1.17	4.34	0.052	2.17	63.5
	1993/04/03	0.80	2.73	0.056	1.56	74.0
	1993/10/31	1.41	5.79	0.041	2.17	67.3
	1993/11/21	1.45	6.93	0.026	2.17	47.6
R Lmi	1992/03/28	2.70	7.55	0.105	−1.30	55.5
	1992/04/23	0.90	2.93	0.130	−1.30	61.8
	1992/05/23	0.47	0.71	0.090	−0.43	35.5
	1992/12/05	2.07	7.71	0.109	−1.73	48.8
	1992/12/27	1.32	5.00	0.153	−1.30	73.2
	1993/01/22	0.35	1.39	0.057	−0.43	77.8
	1993/02/24	0.67	2.69	0.080	−0.43	75.0
	1993/04/03	0.34	0.90	0.065	−0.43	71.6
	1993/10/09	0.59	3.12	0.045	1.30	43.9
	1993/10/31	0.85	3.30	0.041	−0.43	55.1
R Leo	1992/04/23	11.06	32.51	0.099	−1.30	64.6
	1992/05/23	6.14	17.65	0.143	−1.30	31.2
	1992/10/31	17.49	79.59	0.081	−1.27	38.2
	1992/12/05	45.02	174.07	0.083	−0.12	54.8
	1992/12/27	25.93	101.52	0.119	−0.43	63.7
	1993/01/22	15.14	49.79	0.071	−0.43	64.5
	1993/02/24	15.11	55.25	0.080	−0.43	64.3
	1993/04/03	16.18	53.75	0.066	−1.07	34.3
	1993/10/09	8.96	38.21	0.048	−2.17	52.3
	1993/10/31	15.27	66.51	0.045	−1.30	59.1
	1993/11/21	8.80	38.00	0.053	−1.30	45.3

IV. RESULTS

In this study, we have observed ~ 80 long period variables in $v = 1, J = 2 - 1$ SiO emission with 14m radio telescope at DRAO. We have detected 15 previously known emitters, whose periods of light variation are all longer than 300 days. The asymmetric factor derived from the optical curve and IR colors, $log(S_\lambda(12\mu m)/S_\lambda(25\mu m))$ and $log(S_\lambda(25\mu m)/S_\lambda(60\mu m))$ do not indicate any relation with this maser emission by showing no difference between the detected and non-detected maser sources. For T Cep, μ Cep, u Her, R Leo, R Lmi, U ori, and R Ser among them, the time variation of this maser line is compared with the optical light curve(Mattei 1993) at the same time of maser observation. Except for U Ori which is the only one consistently shown ~ 0.2 phase lag, no systematic relation between the maser variation and the optical light curve is found for these stars.

We do not find enough evidences that the SiO maser is directly related with the radiation from the central star. The small amounts of the variation of the velocity at the peak intensity and random distribution of the peak velocity are consistent with the fact that the SiO maser region is confined to a small region and it is not related to the expansion velocity.

Our result is in contradiction with the assumption that the radiation from a central star is a major source for the SiO maser pumping, but it is in line with the notion that in general, collision is more important than radiation for pumping the SiO maser.

ACKNOWLEDGEMENTS

REFERENCES

Alcolea, J., & Bujarrabal, V., 1992, AA, 253, 475

Bieniek, R. J., & Green, S. 1983, ApJ, 265, L29

Bowers, P. F. 1975, AA, 39, 473

Bujarrabal, V., Plareras, P., & del Romero, A. 1987, AA, 175, 164

Cernicharo, J., & Bujarrabal, V., 1992, ApJ, 401, L109

Cernicharo, J., Bujarrabal, V., & Santaren, J., L., 1993, ApJ, 407, L33

Clark., F, D., Troland, T. H., & Johnson, D. R. 1982, ApJ, 261, 569

Colomer, F., Graham, D. A., Kirichbaum, T. P., Rönnäng, B. O., de Vicente, P., Witzel, A., Baudry, A., Booth, R. S., Gómez-González, J., Alcolea, J., & Daigne, G., 1992, AA, 254, L17

Dickinson, D. F., Reid, M. J., Morris, M., & Redman R. 1978, ApJ, 220, L113

Hjalmarson, Å., & Olofsson, H., ApJ, 234, L199

Hollis, J. M., Wright, M. C. H., Welch, W. J., Jewell, P. R., Crull, H. E. Jr., Kafatos, M., & Michalitsianos, A. G., 1990, ApJ, 361, 663

Jewell, P. R., Snyder, L. E., Walmsley, C. M., Wilson, T. L., & Gensheimen, P. D. 1991, AA, 242, 211

Kwan, J., & Scoville, N. 1974, ApJ, 194, L97

Kim, E., & Lee, S. G. 1994, Pub. Kor. Ast. Soc. 8, 83 in Korean

Lockett, P., & Elitzur, M. 1992, ApJ, 399, 704

Mattei, J. A., 1993, Observations from the AAVSO Internatinal Database, private communication

Martinez, A., Bujarrabal, V., & Alcolea, J. 1988, AAS, 74, 273

Moran, J. M., Ball, J. A., Predmore, C. R., Lane, A. P., Huguenin, G. R., Reid, M. J., & Hansen, S. S., 1979, ApJ, 231, L67

Nyman, L., Å., & Olofsson, H., 1985, AA, 147, 309

——————————————————., 1986, AA, 158, 67

Onaka, T., de Jong, T., & Willems, F. J. 1989, AA, 218, 169

Synder, L. E., & Buhl, D. 1974, ApJ, 189, L31